

## Short communication

The effect of fluoride ions on the structure and crystallization kinetics of  $\text{La}_2\text{O}_3$ -containing diopside based oxyfluoride glassesIshu Kansal<sup>a</sup>, Ashutosh Goel<sup>a</sup>, Dilshat U. Tulyaganov<sup>b</sup>, Essam R. Shaaban<sup>c</sup>,  
Manuel J. Ribeiro<sup>d</sup>, José M.F. Ferreira<sup>a,\*</sup><sup>a</sup>Department of Ceramics and Glass Engineering, University of Aveiro, CICECO, 3810-193 Aveiro, Portugal<sup>b</sup>State Committee of Geology and Mineral Resources, Centre of Remote Sensing and GIS Technologies, 11-A, Shevchenko str., 100060, Tashkent, Uzbekistan<sup>c</sup>Physics Department, Faculty of Science, Al-Azhar University, Assuit 71542, Egypt<sup>d</sup>UIDM, ESTG, Polytechnic Institute of Viana do Castelo, 4900 Viana do Castelo, Portugal

Received 3 February 2009; received in revised form 17 March 2009; accepted 14 April 2009

Available online 21 May 2009

## Abstract

Oxyfluoride glasses in the system  $\text{CaO-MgO-BaO-SiO}_2\text{-Al}_2\text{O}_3\text{-La}_2\text{O}_3\text{-CaF}_2$  were obtained by adding  $\text{CaF}_2$  (3–8 wt%) to a parent diopside based glass composition,  $\text{Ca}_{0.8}\text{Ba}_{0.1}\text{MgAl}_{0.1}\text{La}_{0.1}\text{Si}_{1.9}\text{O}_6$ . The characterization of the glasses has been made by density, dilatometry and FTIR measurements. Non-isothermal crystallization kinetic studies in conjunction with XRD and SEM have been employed in order to investigate the effects of fluoride ion additions on crystallization behaviour and mechanism of glasses.

© 2009 Elsevier Ltd and Techna Group S.r.l. All rights reserved.

Keywords: D. Glass; D. Glass-ceramics; D. Silicate; D. Halide;  $\text{CaF}_2$ 

## 1. Introduction

Oxyfluoride-aluminosilicate glasses and glass-ceramics (GCs) have received a great deal of attention in the recent past due to their wide range of applications in different technological areas [1–4]. Oxyfluoride GCs doped with rare earth (RE) ions have been researched widely in the past few decades, since they possess not only higher chemical and mechanical stability than fluoride glass but also lower phonon energy than oxide glass [5]. The GCs of this kind usually contain such small crystalline phases as the nano-size  $\text{Pb}_x\text{Cd}_{1-x}\text{F}_2$  or  $\text{PbF}_2$  crystals in the glass hosts that they can improve the optical properties with no loss of transparency [5–7]. However, both  $\text{CdF}_2$  and  $\text{PbF}_2$  are poisonous so that they cannot be used extensively. Some researchers have developed GCs containing  $\text{LaF}_3$  or  $\text{CaF}_2$  nanocrystals [8–10]. The alkaline-earth fluoride lattice consists of a body-centered (fluorite) cubic structure. The  $\text{F}^-$  ions form a cubic cage with the alkaline-earth cation residing at the centre of each alternate

cage. Trivalent RE ions can be substituted for the divalent alkaline-earth cation [11]. This brings possibilities of preparing transparent GCs containing  $\text{MF}_2\text{:RE}^{3+}$  ( $\text{M} = \text{Mg}^{2+}, \text{Ca}^{2+}, \text{Sr}^{2+}$ , and  $\text{Ba}^{2+}$ ) nanocrystals.

Recently, Sroda and Paluszkievicz [3] investigated the effect of alkaline-earth ions on the structure of oxyfluoride-aluminosilicate glasses. Previously, Agathopoulos et al. [12] had investigated the structural behaviour of the  $\text{CaO-MgO-SiO}_2\text{-CaF}_2$  glasses. However, the amount of  $\text{CaF}_2$  was almost constant in all the investigated glasses. According to the best of our knowledge, no study pertaining to the influence of fluoride ions on the structure and crystallization kinetics of the RE-doped pyroxene-based glasses has been reported so far. Therefore, the present study is an attempt to fill in this lacuna. Three glass compositions have been prepared by adding different amounts of  $\text{CaF}_2$  (3, 5 and 8 wt%, respectively) in the  $\text{La}_2\text{O}_3$ -containing diopside based parent glass composition,  $\text{Ca}_{0.8}\text{Ba}_{0.1}\text{MgAl}_{0.1}\text{La}_{0.1}\text{Si}_{1.9}\text{O}_6$  [13]. The glasses have been labelled according to the amount of  $\text{CaF}_2$ , i.e. parent glass ( $\text{Ca}_{0.8}\text{Ba}_{0.1}\text{MgAl}_{0.1}\text{La}_{0.1}\text{Si}_{1.9}\text{O}_6$ ) will be labelled as 7–0 (0 wt%  $\text{CaF}_2$ ). Similarly, glasses with 3 and 8 wt%  $\text{CaF}_2$  will be labelled as 7–3 and 7–5, respectively. The results pertaining to the parent glass composition (7–0) have been already published

\* Corresponding author. Tel.: +351 234 370242; fax: +351 234 370204.

E-mail address: [jmf@ua.pt](mailto:jmf@ua.pt) (J.M.F. Ferreira).

elsewhere [13] but will be presented and discussed along the manuscript for the convenience of the readers.

## 2. Experimental

Powders of technical grade  $\text{SiO}_2$  (purity > 99.5%) and  $\text{CaCO}_3$  (>99.5%), and of reactive grade  $\text{BaCO}_3$ ,  $\text{Al}_2\text{O}_3$ ,  $\text{MgCO}_3$ ,  $\text{La}_2\text{O}_3$ ,  $\text{NiO}$  and  $\text{CaF}_2$  were used. In order to be consistent with our previous investigation [13], 1 wt% of  $\text{NiO}$  was added to all the three glass batches. Homogeneous mixtures of batches (~100 g), obtained by ball milling, were calcined at 900 °C (1173 K) for 1 h and then melted in Pt-crucibles at 1550 °C (1823 K) for 1 h. Glasses in bulk form were produced by pouring the melts on preheated bronze moulds followed by annealing at 550 °C (823 K) for 1 h.

Dilatometry measurements were done on prismatic samples with a cross section of 4 mm × 5 mm (Bahr Thermo Analyze DIL 801 L, Hüllhorst, Germany; heating rate 5 K min<sup>-1</sup>). A minimum of 3 samples for each composition was analyzed. Glass transition temperature ( $T_g$ ), softening point ( $T_s$ ) and CTE were obtained in the permissible limits of experimental errors.

Infrared spectra for the glasses were obtained using an Infrared Fourier spectrometer (FT-IR, model Mattson Galaxy S-7000, USA). For this purpose samples were crushed to powder form in agate pestle-mortar, mixed with KBr in the proportion of 1/150 (by weight) and pressed into a pellet using a hand press.

Archimedes' method (i.e. immersion in diethyl phthalate) was employed to measure the apparent density of the bulk-annealed glasses and resultant GCs. The mean values and the SD presented for density have been obtained from (at least) 10 different samples.

In order to investigate the crystallization kinetics bulk-annealed glasses were crushed into powder form by hand using agate pestle-mortar. The mean particle size of the glass powders as determined by light scattering technique (Beckman Coulter LS 230, CA USA; Fraunhofer optical model) was in the range 180–250 μm. Crystallization kinetics of the glasses was studied by using differential thermal analysis (DTA, Netzsch 402 EP, Germany). The glass powder weighing 50 mg was contained in an alumina crucible and the reference material was α-alumina powder. The samples were heated in air from ambient temperature to 1000 °C (1273 K) at different heating rates ( $\beta$ ) in the range of 5–20 K min<sup>-1</sup>.

The crystallization behaviour of the glasses was investigated by heat treating the small pieces of bulk glasses in an electric furnace, in air, in accordance with the following thermal cycles: (1) room temperature (RT) → 700 °C (973 K) for a dwell time of 1 h at 700 °C; (2) room temperature (RT) → 800 °C (1073 K) for a dwell time of 1 h at 800 °C; (3) RT → 900 °C (1173 K) for a dwell time of 1 h at 900 °C; (4) RT → 1000 °C (1273 K) for a dwell time of 1 h at 1000 °C; (5) RT → 600 °C (873 K) for a dwell time of 2 h at nucleating temperature ( $T_n$ ), i.e. 600 °C, and then 600 → 900 °C for a dwell time of 1 h at 900 °C; (6) RT → 700 °C (973 K) for a dwell time of 2 h at nucleating temperature, i.e. 700 °C, and then 700 → 900 °C for a dwell time of 1 h at 900 °C. The heating rate in all the thermal cycles was 5 K min<sup>-1</sup>. The crystalline phases were determined on the powdered (crushed by hand using agate pestle-mortar) GCs by X-ray diffraction analysis (XRD, Cu Kα<sub>1</sub> radiation, Bruker AXS, D8 Advance, Germany; 2θ angle range 10–80°; step 0.02 degs<sup>-1</sup>). Micro-structure observations were done at polished (mirror finishing) and then etched (by immersion in 2 vol.% HF solution for 2 min) surfaces of GCs by field emission scanning electron microscopy (FE-SEM, Hitachi S-4100, Japan; 25 kV acceleration voltage, beam current 10 μA) under secondary electron mode.

## 3. Results and discussion

All the glasses obtained after melting were XRD amorphous, which was also confirmed by SEM analysis, afterwards. The density of the glasses varied between 3.08 and 3.12 g cm<sup>-3</sup> and was found to increase with an increase in  $\text{CaF}_2$  content in the glasses (Table 1). The density values of all the investigated glasses are higher than those of BaO- and ZnO-containing diopside-Ca-Tschermak glasses [14,15]. The molar volume ( $V_m$ ) and excess molar volume ( $V_e$ ) were calculated using the apparent density data for the bulk glasses using the relations that have already been reported in our previous work [13–15]. The values of  $V_m$  and  $V_e$  decreased with an increase in  $\text{CaF}_2$  content in the glasses (Table 1). This decrease in  $V_m$  and  $V_e$  may be attributed to the high ionic character of  $\text{CaF}_2$ . Since, the ionic bonds are non-directional in nature, increasing  $\text{CaF}_2$  will lead to the collapse of the structural skeleton into a closer packing, thus, decreasing the excess volume ( $V_e$ ) [16] and, therefore, increasing the CTE of the glasses (Table 1). The values of  $V_m$ ,

Table 1  
Properties of the glasses.

Glass	7-0	7-3	7-5	7-8
Density (g cm <sup>-3</sup> )	3.08 ± 0.001	3.10 ± 0.003	3.11 ± 0.002	3.12 ± 0.005
$V_m$ (cm <sup>3</sup> mol <sup>-1</sup> )	19.71 ± 0.012	19.70 ± 0.014	19.72 ± 0.010	19.60 ± 0.020
$V_e$ (cm <sup>3</sup> mol <sup>-1</sup> )	0.24 ± 0.012	0.11 ± 0.02	0.063 ± 0.012	-0.18 ± 0.036
$T_g$ (±2) (K)	958	930	890	865
$T_s$ (±5) (K)	989	968	959	950
CTE × 10 <sup>6</sup> (K <sup>-1</sup> ) (200–500 °C)	8.69 ± 0.01	8.69 ± 0.05	8.87 ± 0.04	9.31 ± 0.06
$T_p$ (± 2) (K)	1185	1181	1168	1148
$n$	–	2.08 ± 0.01	1.98 ± 0.005	1.94 ± 0.002
$E_c$ (kJ mol <sup>-1</sup> )	300	328	339	342

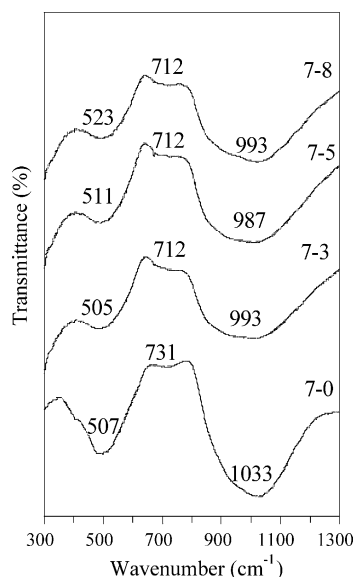


Fig. 1. FTIR spectra of the investigated glass powders.

as obtained for all the glasses under investigation, are lower than their  $B_2O_3$ -containing analogues investigated in our recent study [17]. This is due to the fact that unlike  $CaF_2$ ,  $B_2O_3$  is covalent in nature and thus, promotes directional bonding in the glass structural network.

The room temperature FTIR transmittance spectra of all the investigated glasses are shown in Fig. 1. All spectra exhibit three broad transmittance bands in the region of 300–1300  $cm^{-1}$ . This lack of sharp features is indicative of the general disorder in the silicate network mainly due to a wide distribution of  $Q_n$  (polymerization in the glass structure, where  $n$  denotes the number of bridging oxygens) units occurring in these glasses. The most intense bands in the 800–1300  $cm^{-1}$  region correspond to the stretching vibrations of the  $SiO_4$  tetrahedron with a different number of bridging oxygen atoms while bands in the 300–600  $cm^{-1}$  region are due to bending vibrations of Si–O–Si and Si–O–Al linkages [18,19]. The least intensive bands in the region 650–800  $cm^{-1}$  are related to the stretching vibrations of the Al–O bonds with  $Al^{3+}$  ions in fourfold coordination [18]. The transmittance bands in 800–1300  $cm^{-1}$  region for  $CaF_2$ -containing glasses are registered at considerably lower wave numbers than those observed for  $CaF_2$ -free parent glass (7-0). Thus, it is evident that the introduction of fluoride ions breaks up  $Q_3$  units and favours the formation of  $Q_2$  units. This depolymerization of glass network and formation of NBOs leads to decrease in the  $T_g$  of glasses (Table 1). The band in the region 650–800  $cm^{-1}$  shifted towards lower wave number with the addition of  $CaF_2$ . This may be due to the overlapping of band corresponding to the stretching vibrations of Al–O binds with that of  $F^-$  as the characteristic band for  $F^-$  lies around  $\sim 740\text{ cm}^{-1}$  [20].

The DTA plots of all the  $CaF_2$ -containing glasses exhibit single exothermic effects at all the heating rates which shifted towards higher temperatures with increase in heating rate. The existence of a single crystallization exotherm signifies that either the GC formed as a result of crystallization is mono-

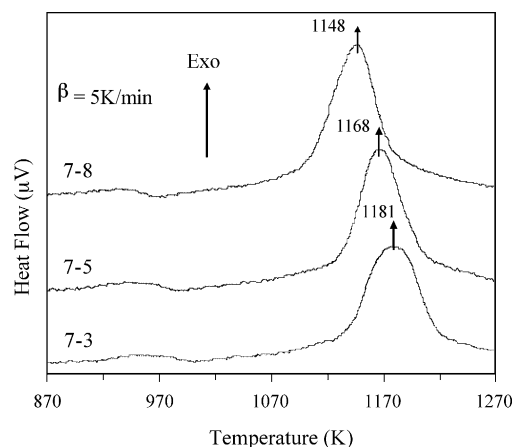


Fig. 2. Differential thermal analysis thermograph of the glasses at  $\beta = 5\text{ K min}^{-1}$ .

mineral or different crystalline phases appear from the glass matrix almost simultaneously and the crystallization curve is the resultant of all the crystallization curves formed due to the appearance of different crystalline phases. The peak temperature of crystallization,  $T_p$  decreased with an increase in  $CaF_2$  content in the glasses as shown in Fig. 2. XRD results of the heat treated glasses reveal that addition of  $CaF_2$  in the parent glass,  $Ca_{0.8}Ba_{0.1}MgAl_{0.1}La_{0.1}Si_{1.9}O_6$  disturbed the formation of pyroxene solid solution and led to the crystallization of diopside (ICDD card: 01-078-1390;  $CaMgSi_2O_6$ ) and  $La_2O_3$ -containing crystalline phase named, britholite (01-076-0340;  $La_{9.31}(Si_{1.04}O_4)_6O_2$ ) in all the thermal cycles except that of heat treatment at 800 °C. All the investigated glasses were amorphous after heat treatment at 800 °C. No fluorine containing phase could be detected after any thermal treatment evidencing that the  $F^-$  ions were accumulated in the glassy phase. Fig. 3a shows the microstructural image of glass 7–8 after heat treatment at 700 °C (step 1) and presents a clear evidence of phase separation in the glasses in the form of network like structures with the introduction of fluoride ions in the glasses. The tendency to form such structures increased with an increase in the concentration of fluoride ions. Further, after heat treatment at 800 °C (step 2) (Fig. 3b), though the glasses were XRD amorphous, nucleation occurred on the edge of the glasses through rosette morphology, evidencing the initiation of surface nucleation. Fig. 3c shows the initiation of crystallization from the surface of sample signifying the presence of surface crystallization while Fig. 3d shows the existence of crystalline phases with different microstructure in the GCs confirming the XRD results. Also, it is noteworthy that all the obtained GCs had either an amorphous glass or a hollow cavity in the core of the GC, thus pointing towards the existence of surface crystallization mechanism. The heating of glasses at different nucleating temperatures (step 4 and step 5) followed by heating them at final crystallization temperature was also ineffective in achieving three-dimensional bulk crystallization in any of the investigated glass compositions. The crystallization kinetics of the  $CaF_2$ -containing glasses was studied using the formal theory of transformation kinetics as developed by Johnson and Mehl [21] and Avrami [22], for non-isothermal

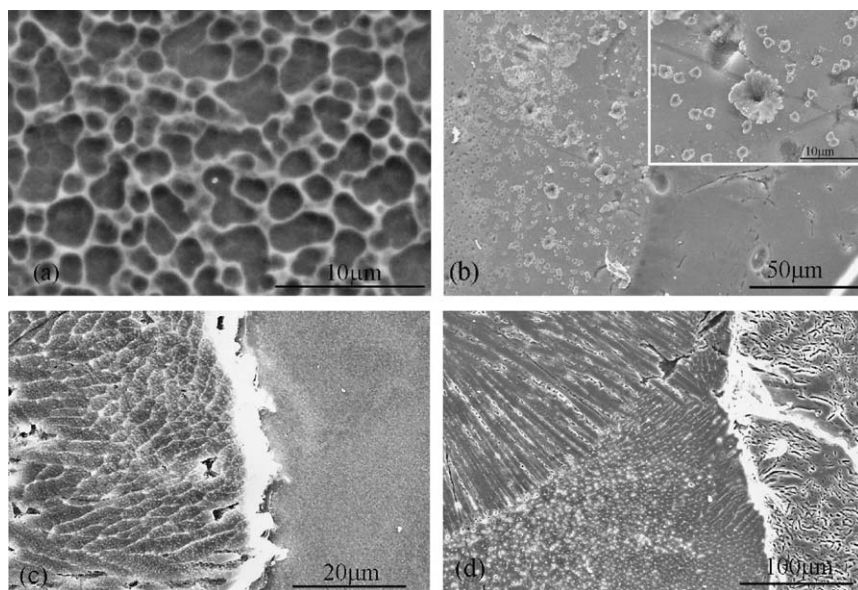


Fig. 3. Microstructure of the glass-ceramics (a) 7-8 (step 1) (a) 7-5 (step 2), (b) 7-3 (step 5) (c) 7-5 (step 6).

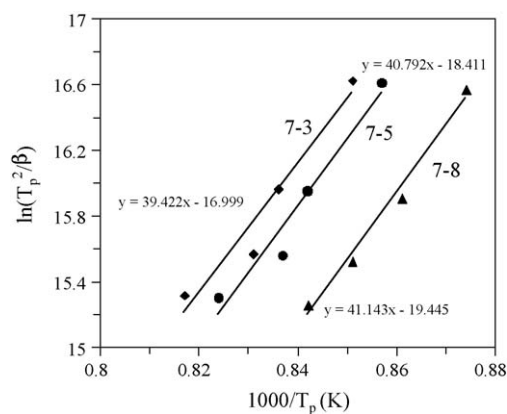


Fig. 4. Plot of  $E_c$  for all the investigated glasses.

processes that have already been obtained in our previous work [23,24]. The Avrami parameters for all the three  $\text{CaF}_2$ -containing glasses were calculated to be in the range 1.93–2.0 (Table 1), signifying towards the two-dimensional crystal growth and intermediate (i.e. simultaneous surface and bulk crystallization) mechanism of crystallization. The activation energy of crystallization ( $E_c$ ) increased with addition of  $\text{CaF}_2$  in the parent glass (7-0) and varied between 300–342  $\text{kJ mol}^{-1}$  (Table 1, Fig. 4).

#### 4. Conclusion

In conclusion, effect of  $\text{CaF}_2$  addition has been investigated on the structure and crystallization behaviour of  $\text{La}_2\text{O}_3$ -containing diopside based glasses. The  $V_m$ ,  $V_e$  and  $T_g$  decreases while density and CTE increases with an increase in fluoride ion content. The addition of fluoride ion causes the silicate glass network to break and thus led to the formation of  $\text{Q}_2$  units. The addition of  $\text{CaF}_2$  disturbed the solid solution formation and led

to the formation of diopside and britholite. Three-dimensional bulk crystallization could not be achieved in any of the  $\text{CaF}_2$ -containing glasses. The  $E_c$  increased with addition of  $\text{CaF}_2$ .

#### Acknowledgements

This study was financially supported by University of Aveiro, CICECO and FCT, Portugal (SFRH/BD/37037/2007).

#### References

- [1] A. Clifford, R. Hill, Apatite-mullite glass-ceramics, *J. Non-Cryst. Solids* 196 (1996) 346–351.
- [2] H. Fathi, A. Johnson, R. van Noort, J.M. Ward, The influence of calcium fluoride ( $\text{CaF}_2$ ) on biaxial flexural strength of apatite-mullite glass-ceramic materials, *Dent. Mater.* 21 (2005) 846–851.
- [3] M. Sroda, Cz. Paluszkiwicz, The structural role of alkaline earth ions in oxyfluoride aluminosilicate glasses—Infrared spectroscopy study, *Vib. Spec.* 48 (2008) 246–250.
- [4] M.J. Dejneka, Transparent oxyfluoride glass ceramics, *MRS Bull.* 23 (1998) 57–62.
- [5] X. Qiao, X. Fan, M. Wang, Luminescence behavior of  $\text{Er}^{3+}$  in glass ceramics containing  $\text{BaF}_2$  nanocrystals, *Scripta Mater.* 55 (2006) 211–214.
- [6] G. Dantelle, M. Mortier, D. Vivien, G. Patriarche, Effect of  $\text{CeF}_3$  addition on the nucleation and up-conversion luminescence in transparent oxyfluoride glass-ceramics, *Chem. Mater.* 17 (2005) 2216–2222.
- [7] G. Dantelle, M. Mortier, D. Vivien, G. Patriarche, Nucleation efficiency of erbium and ytterbium fluorides in transparent oxyfluoride glass-ceramics, *J. Mater. Res.* 20 (2005) 472–481.
- [8] M.J. Dejneka, The luminescence and structure of novel transparent oxyfluoride glass-ceramics, *J. Non-Cryst. Solids* 239 (1998) 149–155.
- [9] S. Tanabe, H. Hayash, T. Hanada, N. Onodera, Fluorescence properties of  $\text{Er}^{3+}$  ions in glass ceramics containing  $\text{LaF}_3$  nanocrystals, *Opt. Mater.* 19 (2002) 343–349.
- [10] J. Fu, J.M. Parker, P.S. Flower, R.M. Brown,  $\text{Eu}^{2+}$  ions and  $\text{CaF}_2$ -containing transparent glass-ceramics, *Mater. Res. Bull.* 37 (2002) 1843–1849.
- [11] J.R. Wells, R.J. Reeves, Optical transitions of  $\text{Er}^{3+}$  ions in fluorozirconate glass, *Phys. Rev. B* 27 (1983) 6635–6648.

- [12] S. Agathopoulos, D.U. Tulyaganov, J.M.G. Ventura, S. Kannan, A. Saranti, M.A. Karakassides, J.M.F. Ferreira, Structural analysis and devitrification of glasses based on the CaO–MgO–SiO<sub>2</sub> system with B<sub>2</sub>O<sub>3</sub>, Na<sub>2</sub>O, CaF<sub>2</sub> and P<sub>2</sub>O<sub>5</sub> additives, *J. Non-Cryst. Solids* 352 (2006) 322–328.
- [13] A. Goel, D.U. Tulyaganov, V.V. Kharton, A.A. Yaremchenko, J.M.F. Ferreira, The effect of Cr<sub>2</sub>O<sub>3</sub> addition on crystallization and properties of La<sub>2</sub>O<sub>3</sub>-containing diopside glass-ceramics, *Acta Mater.* 56 (2008) 3065–3076.
- [14] A. Goel, D.U. Tulyaganov, I.K. Goel, E.R. Shaaban, J.M.F. Ferreira, Effect of BaO on the crystallization kinetics of glasses along the diopside–Ca–Tscheramak join, *J. Non-Cryst. Solids* 355 (2009) 193–202.
- [15] A. Goel, D.U. Tulyaganov, E.R. Shaaban, R.N. Basu, J.M.F. Ferreira, Influence of ZnO on the crystallization kinetics and properties of diopside–Ca–Tscheramak based glasses and glass-ceramics, *J. Appl. Phys.* 104 (2008) 043529.
- [16] J.W. Martin, *Concise Encyclopedia of the Structure of Materials*, Elsevier Science Ltd., UK, 2006, , ISBN: 978-0-08-045127-5.
- [17] A. Goel, D.U. Tulyaganov, V.V. Kharton, A.A. Yaremchenko, S. Eriksson, J.M.F. Ferreira, Optimizaton of La<sub>2</sub>O<sub>3</sub>-containing diopside based glass-ceramic sealant for fuel cell applications, *J. Power Sources* 189 (2009) 1032–1043.
- [18] J.T. Kohli, R.A. Condratr, J.E. Shelby, Raman and Infrared spectra of rare earth aluminosilicate glasses, *Phys. Chem. Glasses* 34 (1993) 81–87.
- [19] L. Stoch, M. Sroda, Infrared spectroscopy in the investigation of oxide glasses structure, *J. Mol. Struct.* 511–512 (1999) 77–84.
- [20] S. Kannan, J.M. Ventura, J.M.F. Ferreira, In situ formation and characterization of fluorine-substituted biphasic calcium phosphate ceramics of varied F-HAP/β-TCP ratios, *Chem. Mater.* 17 (2005) 3065–3068.
- [21] W.A. Johnson, K.F. Mehl, Reaction kinetics in processes of nucleation and growth, *Trans. Am. Inst. Mining Eng.* 135 (1939) 416.
- [22] M. Avrami, Granulation phase change and microstructure-kinetics of phase change III 9 (1941) 177–184.
- [23] A. Goel, E.R. Shabaan, F.C.L. Melo, M.J. Ribeiro, J.M.F. Ferreira, Non-isothermal crystallization kinetics of MgO–Al<sub>2</sub>O<sub>3</sub>–SiO<sub>2</sub>–TiO<sub>2</sub> glass, *J. Non-Cryst. Solids* 353 (2007) 2383–2391.
- [24] A. Goel, E.R. Shabaan, F.C.L. Melo, M.J. Ribeiro, J.M.F. Ferreira, Influence of NiO on the crystallization kinetics of near stoichiometric cordierite glasses nucleated with TiO<sub>2</sub>, *J. Phys. Condens. Matter.* 19 (2007) 386231.